Published in final edited form as:
J Neurosci. 2013 April 24; 33(17): 7384–7392. doi:10.1523/JNEUROSCI.5839-12.2013.

Zebrafish calls for reinterpretation for the roles of P/Q calcium channels in neuromuscular transmission

Hua Wen[1,3], **Michael W. Linhoff**[1], **Jeffrey M. Hubbard**[1], **Nathan R. Nelson**[1], **Donald Stensland**[3], **Julia Dallman**[4], **Gail Mandel**[1,2,3], and **Paul Brehm**[1,3]

[1]Oregon Health and Science University, 3181 S.W. Sam Jackson Park Rd, Portland, Oregon, 97239.

[2]Howard Hughes Medical Institute.

[3]Department of Neurobiology and Behavior, SUNY at Stony Brook, Stony Brook, New York 11794.

[4]Department of Biology, University of Miami, Coral Gables, Florida 33124.

Abstract

A long-held tenet of neuromuscular transmission is that calcium-dependent neurotransmitter release is mediated by N-type calcium channels in frog but P/Q-type channels in mammals. The N-type assignment in frog is based principally on pharmacological sensitivity to ω-conotoxin GVIA. Our studies show that zebrafish neuromuscular transmission is also sensitive to ω-conotoxin GVIA. However, positional cloning of a mutant line with compromised neuromuscular function identified a mutation in a P/Q- rather than N-type channel. Cloning and heterologous expression of this P/Q-type channel confirmed a block by ω-conotoxin GVIA raising the likelihood that all vertebrates, including frog, utilize the P/Q-type calcium channel for neuromuscular transmission. Additionally, our P/Q defective mutant line offered a means of testing the ability of roscovitine, known to potentiate frog neuromuscular transmission, to mediate behavioral and functional rescue. Acute treatment led to rapid improvement of both, pointing to potential therapeutic benefit for myasthenic disorders involving calcium channel dysfunction.

Keywords

Conotoxin; roscovitine; motor neuron; myasthenia; ion channel

Introduction

The role played by voltage-dependent calcium channels in neural transmission has been the subject of intense investigation since first studied at the frog neuromuscular junction (NMJ, Katz and Miledi, 1967). Of particular significance has been the distinction between the calcium channel isoforms mediating synaptic transmission at certain peripheral and central synapses. Instrumental to this assignment were the toxins that blocked N- and P/Q-types, the major mediators of presynaptic calcium entry. Numerous studies have also suggested, somewhat surprisingly, that different isoforms mediate neuromuscular transmission in different classes of vertebrates. L-type calcium channels were reported for lizard (Lindgren

Corresponding Author: Paul Brehm Oregon Health & Science University 3181 S.W. Sam Jackson Park Rd. Portland, OR 97239 brehmp@ohsu.edu Fax: 503-418-1624.

The authors declare no competing financial interests.

and Moore, 1989), N-type for frogs (Sano et al., 1987; Katz et al., 1995) and *Xenopus* (Thaler et al., 2001) and P/Q-type for mammals (Uchitel et al., 1992). For both *Xenopus* and lizard minor contributions by L- or N-types have been noted, potentially reflecting a mixture of channel types (Hulsizer et al., 1991; Thaler et al., 2001; Lindgren and Moore, 1989). Similarly, N-type channels have been reported for developing mammalian neuromuscular synapses (Siri and Uchitel, 1999) and P/Q-type channels at the adult frog NMJ (Nurullin et al., 2011), respectively. These isolated reports notwithstanding, the fact remains that the principal isoforms responsible for neuromuscular transmission are considered to differ for the three classes of vertebrates studied to date, and these differences have been used to provide support for the specificity of the toxins used in mammals.

The calcium channel isoform mediating neuromuscular transmission in fish remains an open question, but zebrafish is ideally suited to address this question due to the combination of paired motor neuron-target muscle recording technique (Wen and Brehm, 2005; 2010) and our identification of a calcium channel mutant line with greatly compromised synaptic transmission. Using paired nerve-muscle recordings we found that, as it is in frogs, evoked release at the NMJ is effectively blocked by ω-conotoxin GVIA, pointing to a N-type channel as the principle mediator of neuromuscular transmission in zebrafish. However, positional cloning from the zebrafish mutant line *tb204a* identified a mutation in a P/Q-type calcium channel as responsible for compromised neuromuscular transmission. Cloning and pharmacological characterization of the expressed P/Q-type channel further confirmed its unexpected sensitivity to ω-conotoxin GVIA. Given these results and the likely erroneous assignment of N-type to lower vertebrates based on presumed specificity of ω-conotoxin GVIA, a parsimonious resolution is that all vertebrates rely principally on a P/Q-type calcium channel to mediate neuromuscular transmission. With this in mind we used our P/Q mutant line to revisit the actions of the cyclin-dependent kinase (CDK) inhibitor, roscovitine, which was reported to increase transmitter release at the adult frog NMJ (Cho and Meriney, 2006). Our experiments demonstrate that roscovitine rescues both motility defects and neuromuscular transmission in the *tb204a* mutant, a model system relevant to the human myasthenic syndrome involving compromised P/Q-type channel function.

Materials and Methods

In vivo electrophysiological recordings, calcium imaging and motility quantitation

Paired recordings of caudal primary (CaP) motor neuron and fast skeletal muscle from 72-96 hpf (hours post fertilization) fish were performed as described previously (Wen and Brehm, 2005; 2010). The sex of the larval fish was not determined.

For calcium imaging, 100 μM Fluo-5F (green signal, Invitrogen-Molecular Probes) was loaded into the CaP neuron by means of the recording patch pipette. Live confocal images were acquired using a Yokogawa CSU-10 spinning disc (Yokogawa, Tokyo, Japan) with a Stanford Photonics 620 Turbo ICCD camera (Stanford Photonics, Palo Alto, California) and Zeiss Plan-Apochromat 40x/1.0 W objective. For each recording, an acquisition plane was selected to contain 10-15 synaptic boutons in the field. Sequential images were acquired at 33 msec intervals during 100 Hz stimulation. The cumulative calcium signals for each of 10-15 boutons were background subtracted using off-bouton sites. The CaP was also co-loaded with Alexa 647 hydrazide (red signal) to identify the boutons and to normalize the calcium signal as the green/red ratio (ΔG/R). Images were analyzed with ImageJ (NIH, Bethesda, Maryland).

Motility measurements were made by high-speed image acquisition of mechanically induced escape responses. The swimming was recorded at 1000 frames per second using a Fastcam 512-PCI camera (Photron Instruments, San Diego, CA). The duration, frequency and

mechanical bend associated with the swimming were then quantitated using Flote zebrafish motion analysis software (Burgess and Granato, 2007).

Positional cloning and identification of the tb204a gene

Zebrafish heterozygous for *tb204a* (Granato et al., 1996) were out-crossed to Brian's wild type. Bulked segregant analysis was first performed by comparing linkage of genomic DNA isolated from homozygous mutants and siblings to a set of 214 microsatellite markers (https://wiki.zfin.org/display/prot/Bulk+Segregant+Markers). This initial scan established the linkage of the mutation to markers on linkage group 11 (LG11). High-resolution mapping, carried out by designing more LG11 markers, determined that the *tb204a* mutation was tightly linked to two markers, one on BAC BX323548 (1/516 recombinants) and another on BAC CT573143 (1/678 recombinants). cDNAs for the genes predicted near this region were individually derived from both mutants and siblings, and sequenced. A single nucleotide substitution (T4984A) was identified in CACNA1Ab in the homozygous mutants.

Cloning of zebrafish calcium channels

Total RNA was extracted from 72-96 hpf embryos with TRIzol Reagent (Ambion), and used as template for first-strand cDNA synthesis using Superscript III synthesis system for RT-PCR (Invitrogen). Full-length cDNA for the zebrafish CACNA1Ab was amplified with primers: forward: 5′-GCTTTTCTCGAGGACACCATGGCTCGGTTCGGAGACGAAGTGCCGGCC-3′ reverse: 5′-CCACCCGGTACCTTAACACCAATCATCCTCGTCCGTCTCGCT-3′ PCR product was cloned into the pEGFP-C3 vector to tag the channel in-frame with EGFP at the N-terminus. An un-tagged version was also made by removing the EGFP cassette. A 2.7 Kb CACNA1Ab fragment encompassing the mutation at nucleotide position 4984 was amplified from *tb204a* homozygous mutants and swapped into the full-length channel to make the expression vector for CACNA1Ab(Y1662N).

To clone the full-length zebrafish CACNA1Ba cDNA, two overlapping fragments were first amplified using the following primers sets: forward 1: 5-′AATCTGAAGCTTGACACCATGGCTCGCTTCGAAGACGATCTCCCGACC-3′ reverse 1: 5′-GTAGGCAAAGTCACTCCCACACTCC-3′ forward 2: 5′-CGCAGAACCAGCAGTCCTTTCAG-3' reverse 2: 5′-ATTAAAGGATCCCTAGCACCAGTCCTCCACCTCTGCCTCTGG-3′ PCR products were cloned into pEGFP-C3 vector to tag the channel in-frame with EGFP at the N-terminus.

Zebrafish voltage-dependent calcium channel β subunit CACNB4b cDNA was amplified with the following primers and cloned into pCDNA3.1 vector: forward: 5′-TTGGAAGGATCCGCCACCATGTATGACAATTTGTACCTGCATGG-3′ reverse: 5′-GGCCGGGAATTCTCAGAGCCGGTGTCGTGAGTCCTG-3′

All clones were confirmed by DNA sequence analysis. Accession numbers for the zebrafish CACNA1Ab, CACNA1Ba and CACNB4b are KC192783, KC192784 and KC192785, respectively.

Whole cell patch clamp recording of expressed calcium channels

Human embryonic kidney (HEK293T) cells were transfected by Lipofectamine 2000 (Invitrogen) with a mixture containing, in equal molar ratio, cDNAs for the EGFP-tagged α subunit, rat α2δ1 subunit (Addgene, accession number: AF286488) and the zebrafish β4b subunit. To ensure that the EGFP tag does not alter channel properties, untagged channels

were used in some experiments, and yielded indistinguishable results from the tagged channel. To express the un-tagged channel, pEGFP-C3 vector was co-transfected with the channel subunits. 24 hrs after transfection, cells with bright green fluorescence were recorded in the whole cell voltage clamp mode with an EPC9 amplifier (HEKA Elektronik, Lambrecht, Germany). Patch electrodes with resistances of 3-5 MΩ contained (in mM): 115 Cs methanesulfonate, 15 CsCl, 5 BAPTA, 4 Mg-ATP, and 10 HEPES, pH 7.2 with CsOH, ~280 mOsm. The recording bath solution for recording CACNA1Ab currents contained (in mM): 134 NaCl, 2.9 KCl, 1.2 $MgCl_2$, 10 $BaCl_2$, 0.2 $CaCl_2$ and 10 HEPES, pH 7.2 with NaOH, ~ 290 mOsm. 5 mM Ba^{2+} was used as the charge carrier in CACNA1Ab pharmacology experiments, and 1 mM Ba^{2+} was the charge carrier for all CACNA1Ba recordings. 1 μM tetrodotoxin (TTX, Alomone labs, Jerusalum, Israel) was included in the bath solution. Whole-cell currents were sampled at 50 kHz and filtered at 2 kHz with PULSE software (HEKA Elektronik, Lambrecht, Germany). Data were leak-subtracted on-line with a p/10 protocol. We observed an endogenous current in some HEK293T cells that is fast-activating, fast-inactivating and TTX-insensitive. Because of its small size and fast kinetics, it did not interfere with calcium current measurements. Series resistance compensation was performed for cells with current >500 pA. Only cells with series resistance <10 MΩ were used for analysis. In conjunction with the small current size recorded under these conditions, the voltage error is estimated to be small. Data was analyzed with FitMaster and IGOR Pro (WaveMetrics, Lake Oswego, OR). All results were presented as mean ± standard deviation (S.D.). Standard t-test was performed to test for statistical significance between groups.

Drugs

All toxins were obtained from Alomone Labs. ω-conotoxin GVIA, ω-conotoxin MVIIC, ω-Agatoxin IVA were dissolved in water and stored as 100 μM stock solutions at -20°C. The stock solution for ω-Agatoxin TK was 10 μM. Each toxin was diluted to working concentration using recording bath solutions immediately before use and puffer applied to the cell using a pipette with a ~5 μm opening. Roscovitine (Alomone Labs) was applied to fish at 100 μM for 0.5-1 hr before the behavior analysis, and to a paired recording preparation for 20 min before recordings. It was puffer applied to HEK923 cells in a similar manner as in the toxin applications. 3,4-diaminopyridine (DAP, Sigma) was applied at 200 μM for 1 hr before the behavior analysis.

Results

Paired recordings between CaP motor neuron and target fast skeletal muscle were used to determine the calcium channel isoform responsible for evoked release. In control fish, the endplate currents (EPCs) followed motor neuron action potentials without failure during a 1 sec, 100 Hz train (Figure 1A). Over this time period of stimulation the release occurs principally in a synchronous manner (Wen et al., 2011). To test the roles of individual calcium channel isoforms in synaptic release, toxins were applied for 15 minutes prior to the recording. The total charge transfer associated with the postsynaptic currents during the stimulation period was used to quantitate the effects on release. A potential role played by N-type channels was tested first by treatment with 1 μM ω-conotoxin GVIA, a toxin that effectively blocks amphibian neuromuscular transmission (Kerr and Yoshikami, 1984). Treatment with 1 μM ω-conotoxin GVIA nearly abolished postsynaptic muscle EPCs, as reflected in a high failure rate (Figure 1A) and reduced charge transfer (Figure 1B). This pointed to an exclusive role of N-type channels in mediating zebrafish neuromuscular transmission. Further support for a role of N-type channels was provided by 1 μM ω-conotoxin MVIIC, a blocker of both P/Q- and N-type channels in mammals (Figure 1A & 1B). A role of P/Q-type channels in neurotransmission was initially dismissed on the basis

of insensitivity to 2 μM ω-agatoxin IVA (Figure 1A & 1B), a concentration 10 fold higher than needed for block of mammalian P/Q-type channels (Regehr and Mintz, 1994). Comparisons from a large number of paired recordings were made on the basis of total charge entry during the 1 sec recording period. The overall mean values corresponded to 1.4 ± 1.9 pC for ω-conotoxin GVIA (n=13), 22.5 ± 19.8 pC for ω-conotoxin MVIIC (n=5) and 362.8 ± 124.5 pC for ω-agatoxin IVA (n=5), as compared to 301.8 ± 137.6 pC for control recordings (n=15). These results with pharmacology are consistent with the idea that zebrafish NMJ utilizes N-type, instead of P/Q-type calcium channels for synaptic transmission.

To identify and clone the calcium channel isoform responsible for neuromuscular transmission we first searched the zebrafish genome for the pore forming α subunits of N-type calcium channels. This choice was guided by the pharmacologic block of release by ω-conotoxin GVIA, widely considered to be a specific blocker of N-type channels. Two candidate N-type genes were identified based on their homology to vertebrate N-type channels. CACNA1Ba was selected for further study based on a greater sequence similarity to mammalian N-type channels in the II - III loop, which has been shown to mediate interactions with synaptic proteins (Sheng et al., 1996).

We generated a full-length clone for this α subunit and transiently expressed it in HEK293T cells as a fusion protein with GFP. In transfected HEK cells we observed a GFP signal at the cell surface and used it to select high expressing cells for whole cell voltage clamp. Using 1 mM Ba^{2+} as the charge carrier, an inward current was observed in most of these cells, which activated near -20 mV, peaked at 7.5 ± 6.5 mV (n=22) and inactivated slowly during the 100 msec depolarization to +10 mV (Figure 2A & 2B). The Ba^{2+} current was reduced by 97.7 ± 1.3% (n=8) in response to 1 μM ω-conotoxin GVIA (Figure 2C, top panel). 1 μM ω-conotoxin MVIIC was slightly less effective, reducing the current by 87.5 ± 6.1% (Figure 2C, middle panel; n=6). The P/Q-type blocker ω-agatoxin IVA was tested at 2 μM (n=5), a concentration corresponding to 10-fold higher than used to block mammalian P/Q-type calcium channels (Regher and Mintz, 1994). At this concentration the inward current was reduced by 10.9 ± 2.9% (n=5), but the fast onset and recovery yielded the impression that this small reduction might represent an application artifact (Figure 2C, bottom panel). Overall, the pharmacological profile of the expressed N-type isoform was consistent with the profile provided by paired recordings at the NMJ. On the basis of these findings we generated a monoclonal antibody against our candidate N-type channel. Unexpectedly, the antibody failed to effectively label the NMJ of zebrafish, casting doubt on a role played by this channel in neuromuscular transmission. A pan-calcium channel antibody effectively labeled the presynaptic boutons of the CaP motor neuron (data not shown), ruling out the possibility that calcium channel density is too low to be detected by immunohistochemistry *in vivo*.

The identity of the calcium channel isoform mediating zebrafish neuromuscular transmission was ultimately provided by our recent characterization of a motility mutant line, *tb204a* (Granato et al., 1996). This line exhibits a high threshold to mechanically activated escape response. When activated, the initial bend is weak and the swimming bout is brief compared to wild type fish. Paired recordings indicated greatly compromised synchronous transmission as reflected in reduced EPC amplitude and frequent failures, even at frequencies as low as 1 Hz (Figure 3A). The total release during 1 sec, 100 Hz stimulation was reduced from 301.8 ± 137.6 pC in wild type (n=15) to 33.2 ± 18.2 pC in *tb204a* mutant fish (n=9, Figure 3B & 3C). As with wild type fish the residual synaptic transmission was abolished in *tb204a* mutant fish following application of 1 μM ω-conotoxin GVIA (n=3, Figure 3B). To establish that the compromised release resulted from reduced calcium entry we performed two sets of experiments. First, we raised the external calcium concentration

from 2.1 mM to 10 mM and performed paired recordings. During a 1 sec, 100 Hz train the EPC failure rate was significantly reduced at the higher calcium concentration, and total release increased to 75.2 ± 17.8 pC (n=6) indicating a partial functional rescue (Figure 3B & 3D). Second, we directly measured calcium entry into the presynaptic boutons during stimulation in both wild type and mutant fish by *in vivo* calcium imaging. For this purpose calcium indicator dye Fluo-5F was loaded into the motor neurons through the patch pipette. In wild type motor neurons the calcium signal at presynaptic boutons rose quickly during a 100 msec, 100 Hz train, while in mutant boutons the calcium response was greatly reduced (Figure 3E). On average the calcium signal decreased from 4.41 ± 0.33% in wild type to 1.50 ± 0.11% in *tb204a* (Figure 3F).

Evidence for a defective calcium channel causal to the mutant phenotype was provided by positional cloning. The mutation in *tb204a* was mapped to the α subunit of the P/Q-type calcium channel located on chromosome 11 (CACNA1Ab). This gene has been previously annotated as P/Q-type on the basis of sequence similarities to the mammalian homologues (Figure 4B). Zebrafish P/Q-type sequence is more homologous to mammalian P/Q-type than mammalian N-type. Similarly, our cloned zebrafish N-type is more similar to mammalian N-type than mammalian P/Q-type, confirming the assignment. A point mutation from T to A, resulting in a Y1662N substitution in the protein sequence, was located near the intracellular S6 membrane/cytoplasmic interface of Domain IV (Figure 4A). This tyrosine is highly conserved between all N-type, P/Q-type and L-type calcium channels in vertebrates (Figure 4A). RT-PCR analysis of the P/Q-type transcripts from wild type and homozygous mutant fish did not reveal any difference in mRNA expression level or splicing pattern (data not shown). Thus, the single nucleotide substitution likely causes functional differences on the protein level. A zebrafish sensory mutant line (*fakir*) was recently linked to a point mutation in a different region of this P/Q-type channel gene (Low et al., 2012). Consequently, *tb204a* and *fakir* represent different mutant alleles of the same calcium channel gene. Both *tb204a* and *fakir* mutants showed defects in sensory circuitry, as reflected in the reduced touch responsiveness, but our results demonstrate for the first time severely compromised NMJ transmission in zebrafish with P/Q-type calcium channel mutations.

To test the functional consequences of the mutation we cloned the full-length zebrafish P/Q-type channel α subunit, and expressed both mutant and wild type forms in HEK293T cells. The current-voltage relations for whole cell Ba^{2+} current were first determined for wild type P/Q-type calcium channels (Figure 4C & 4D). Unlike the N-type counterpart, this channel expressed at much lower levels requiring elevation of the Ba^{2+} concentration from 1 mM to 10 mM, which also compromised the effectiveness and onset of the toxin block. The decreased functional expression likely reflected a greatly reduced translocation to the cell surface compared to the N-type channel. This was manifest in GFP fluorescence that was trapped inside of the cell. In those cells with measurable current the peak current averaged 241.3 ± 225.6 pA corresponding to a current density of 15.9 ± 14.7 pA/pF (n=20). The inward current for wild type channels activated near -20 mV and peaked at 14.5 ± 4.4 mV with slow inactivation occurring during the 100 msec pulse (Figure 4C & 4D). By contrast, cells expressing the mutant P/Q-type calcium channels usually showed no signs of inward Ba^{2+} current. However, in the infrequent cells showing Ba^{2+} current, the peak current averaged 103.2 ± 63.8 pA corresponding to a current density of 5.1 ± 2.8 pA/pF (n=16). The current activated at -20 mV, similar to wild type channels, but peak activation was shifted to 28.1 ± 3.1 mV in 10 mM Ba^{2+} (Figure 4C & 4D).

The pharmacological profile was next determined for wild type P/Q-type channels expressed in HEK cells in order to compare to the profile obtained for paired recordings *in vivo* (Figure 5). In particular, it was important to resolve the block by ω-conotoxin GVIA

observed *in vivo*, normally reserved for N-type channels. Application of 1 μM ω-conotoxin GVIA in 10 mM Ba^{2+} bath reduced the peak current by 53.4 ± 7.5% (n=10, Figures 5A & 5D). Comparison of the block of expressed channels to *in vivo* paired recordings was complicated by the dependence of block on divalent ion concentration. It has been well established that elevated divalent ion concentration greatly slows the onset and reduces the level of block of calcium channels by toxins in mammalian neurons (McDonough et al., 1996; 2002). Thus, it is likely that the effectiveness of the conotoxin is underestimated in our recordings of the expressed P/Q-type channel owing to the competition between divalent cations and toxin block. Consistent with this idea, when ω-conotoxin GVIA was tested in 5 mM Ba^{2+} bath, a 72.6 ± 10.5% block of peak current along with a more rapid onset was observed (n=6, Figure 5A & 5D). Treatment of 1 μM ω-conotoxin MVIIC reduced the current by 59.4 ± 11.5% (n=10; Figure 5B & 5D). The P/Q-type blocker 2 μM ω-agatoxin IVA yielded variable results, but overall reduced the current by 29.5 ± 16.1% (n=7; Figure 5C & 5D). Another P/Q-type blocker 2 μM ω-agatoxin TK reduced the current by 2.3 ± 2.9% (n=6; Figure 5D). The block of both synaptic transmission and P/Q mediated Ba^{2+} current by ω-conotoxin GVIA support the major role by this calcium channel isoform at zebrafish NMJ. It appears that ω-agatoxin IVA and ω-agatoxin TK are less effective antagonists of zebrafish P/Q-type channels than mammalian counterparts, which is not unexpected. However, ω-agatoxin IVA shows a modest block of the expressed channel but had no obvious effect on synaptic transmission. This may reflect differences in divalent dependence used for synaptic transmission (2 mM Ca^{2+}) and measurement of expressed calcium channels (5 mM Ba^{2+}). Alternatively, a small effect of ω-agatoxin IVA may have gone undetected due to the variability in the release measured during paired recording.

Our results have established that a Y1662N mutation in a zebrafish P/Q-type calcium channel is causal to greatly diminished neuromuscular transmission. Similarly, in patients with Lambert-Eaton syndrome there is reduced synaptic transmission due to compromised P/Q-type calcium channels. However, this stems from a reduction in calcium channel number rather than through altered channel function. In both humans and our mutant zebrafish line the motility is greatly compromised (Figure 6A & 6B) rendering it a good model for evaluating functional and behavioral rescue associated with pharmacological treatment. A standard treatment for patients is the potassium channel blocker DAP. The synaptic improvement is thought to result from increased calcium entry that is associated with prolongation of the action potential. Treatment of *tb204a* fish with 200 μM DAP greatly reduced the number of postsynaptic failures (data not shown). However, there were also spontaneous action potentials occurring along with a variable broadening of the spikes. Improved behavioral rescue was reflected in the ability to mount an effective initial bend followed by swim strokes (Figure 6A & 6B).

Of greater interest was the effect of roscovitine, a CDK inhibitor that augments release at the frog NMJ through slowed deactivation of 'N'-type calcium channels (Cho and Meriney, 2006; Buraei et al., 2007). We performed analogous testing of roscovitine on the wild type zebrafish P/Q-type calcium channels expressed in HEK cells. Application of 100 μM roscovitine resulted in a slight decrease in steady state calcium current along with a pronounced slowing of the calcium tail current in response to voltage steps back to -80 mV from +40 mV. The tail currents were well fit by single exponential functions with mean time constants of 0.43 ± 0.15 msec for pre-treatment and 1.09 ± 0.35 msec for post-roscovitine treatment, corresponding to an average increase of 253.1% ± 29.1% (n=7, Figure 6C). The effects occurred within the 5 sec intervals used for testing the effects on calcium current and were fully reversible.

Next, we took advantage of our unique opportunity to test roscovitine on rescue of neuromuscular function using paired recordings of the mutant line. The *tb204a* mutant fish

are characterized by a low quantal content and high failure rate. However, treatment with roscovitine led to increased EPC amplitude and remarkably improved ability to follow 1 Hz motor neuron firing without failures (Figure 6D). Unlike the action of DAP, this augmentation was not associated with any noticeable change in the action potential waveform. Similar reduction of failure rates and increase of EPC amplitudes were also observed for higher frequency stimulation (Figure 6E), further suggesting an increased presynaptic release probability following drug treatment. Overall, roscovitine treatment increased total release during 1 sec of 100 Hz stimulation to 160 ± 6.2 pC (n=7), significantly greater than the untreated mutants, 33.2 ± 18.2 pC (n=9), and corresponding to about half of that of the wild type level (Figure 6F).

Finally, we turned to testing of roscovitine action on motility using the *tb204a* mutant fish. As with the effects on neuromuscular transmission, 100 μM roscovitine led to remarkable improvement in motility. Quantitation of motility, using motion tracking software, revealed a rescue of both touch responsiveness and swimming behavior within minutes of application (Figure 6A & 6B). In contrast to untreated *tb204a* mutants, these fish responded to a touch stimulus by generating a strong bend of the body axis, followed by alternating bends that propelled them away from the stimulus (Figure 6A & 6B).

Discussion

Our findings underscore the importance of using the sequence information rather than pure pharmacology to assign calcium channel isoforms responsible for mediating neurotransmitter release at a particular synapse. In our case the molecular assignment was rendered using a motility mutant line that exhibited greatly reduced synchronous synaptic transmission. This mutant line, originally designated as *tb204a*, was among the motility mutants that represented a single unresolved allele (Granato et al., 1996). Positional cloning of *tb204a* identified the culprit gene as a P/Q-type calcium channel, contradicting the toxin based pharmacology from *in vivo* paired recordings that pointed to a N-type calcium channel at the zebrafish neuromuscular synapse. Recently, a point mutation in the same calcium channel was identified in *fakir*, another mutant line generated through the Tubingen screen (Granato et al., 1996). *Fakir* was listed among the “reduced touch” mutants whereas *tb204a* was listed among “reduced motility” mutants. *Fakir* and *tb204a* both share a high threshold for evoking mechanically activated swimming and a greatly compromised ability to swim, once activated. Findings from *fakir* pointed to a reduced sensory component (Low et al., 2012), but our results now demonstrate a defect in neuromuscular transmission, accounting for the weak and brief swimming bouts.

The residual transmission in our calcium channel mutant line *tb204a*, observed by means of paired recording, could reflect either a partial loss of function on the part of the mutated P/Q-type calcium channel or the presence of a second ω-conotoxin GVIA sensitive calcium channel isoform. Many studies have revealed mixtures of L- and N-type calcium channels at the NMJ and there is precedence in mammals for mixed N- and P/Q-types at developing NMJ (Urbano et al., 2002; Nurullin et al., 2011). As shown for the mammalian Calyx of Held there is potential for a developmental shift toward P/Q-type channel expression. Should a switch from N-type to P/Q-type occur at zebrafish NMJ it would have to happen at a very early stage of development, as the majority of channels at 96 hpf are P/Q based on our paired recordings from *tb204a*. Additionally, we did not detect any immunohistochemical labeling with our N-type antibody at sites corresponding to NMJs. In the absence of any evidence directly pointing to a second calcium channel isoform, we interpret our findings as a single P/Q isoform governing zebrafish NMJ transmission. Both our heterologous expression and calcium imaging measurements indicate directly that the

missense mutation does not result in a functional null. Instead the calcium entry is compromised by a positive shift in voltage dependence and possibly reduced trafficking.

Based on studies using both frog and *Xenopus*, we expected neuromuscular transmission in zebrafish to be mediated by a N-type calcium channel. However, our unexpected finding for a role of P/Q-type brings the N-type assignment in amphibians into question. The original assignment rested entirely on inhibition by ω-conotoxin GVIA at frog neuromuscular synapse (Sano et al., 1987; Thaler et al., 2001). This toxin has a long history of utility in identifying calcium channels as N-type both in heterologous expression systems and *in vivo*. In 1984 Kerr and Yoshikami first demonstrated its inhibition of neuromuscular transmission at the frog NMJ. The assignment of a N-type channel (Sano et al., 1987) was based on pharmacological profiling of neuronal calcium channels from higher vertebrates, including chick (Kasai et al., 1987) and mammal (McCleskey et al., 1987; Plummer et al., 1989; Regan et al., 1991). Additional confirmation of N-type was provided by effective labeling of active release zones at frog NMJ by fluorescently conjugated ω-conotoxin GVIA (Robitaille et al., 1990). However, evidence that amphibian neuromuscular transmission might utilize a P/Q-type rather than a N-type was reflected in a single study showing sensitivity to both ω-conotoxin GVIA and P-type blocker funnel-web spider toxin (Katz et al., 1995). An inability of ω-conotoxin GVIA to discriminate between N- and P/Q-type channels was also indicated in chick central neurons (Lundy et al., 1994). None-the-less it is clear that mammalian P/Q-type channels are insensitive to ω-conotoxin GVIA. This toxin has no effect on the neuromuscular transmission in either mouse (Sano et al., 1987; Uchitel et al., 1992), humans (Protti et al., 1996) or heterologously expressed mammalian P/Q-type channels (Mori et al., 1991; Ellinor et al., 1994). Therefore, the mixed pharmacology reflected in the zebrafish P/Q-type channel is restricted to non-mammalian vertebrates, and fish likely represent an early divergence of P/Q- and N-type channels. As such, they share the primordial pharmacological profile of being blocked by ω-conotoxins GVIA and MVIIC. In light of these findings, care should be taken when using the frog NMJ to determine toxin specificity. For example, ω-conotoxin CNVIIA, shown to block mammalian N-type channels in rat brain synaptosomes, fails to block frog neuromuscular transmission (Favreau et al., 2001). Instead of representing a new toxin for discriminating between N-type channels, as proposed, another interpretation is that ω-conotoxin CNVIIA represents a N-type blocker that fails to recognize frog P/Q-type channels.

Finally, the identification of a P/Q-type mutant line has aided our understanding of Lambert-Eaton syndrome (LEMS). LEMS represents a human autoimmune myasthenic syndrome that targets P/Q-type channels. In LEMS a reduced calcium entry results from a lowered density of calcium channels whereas *tb204a* represents compromised calcium channel function. Both represent a partial knockdown of function rather than a complete null, so the zebrafish P/Q mutant line provided the first combined electrophysiological and behavioral assessment of human therapeutics. The most common pharmacological treatment used for LEMs patients is DAP, which is predicted to prolong action potentials, thus enhancing presynaptic calcium entry by activating more calcium channels (Quartel et al., 2010). Indeed, raising the calcium concentration to 10 mM partially rescued synaptic transmission in the mutant fish. We found that DAP did improve movement, but also resulted in associated complications due to firing of multiple spikes by the motorneuron in response to stimulation. This uncontrolled firing could potentially interfere with coordination. However, despite the hyperexcitability there was an obvious behavioral improvement in swimming.

We tested next roscovitine, a CDK inhibitor that is used clinically to treat tumors in patients (Senderowicz, 2003). It has also been shown to augment release at adult frog NMJ (Cho and Meriney, 2006) and certain central synapses (Yan et al., 2002; Kim and Ryan, 2010; Tomizawa et al., 2002). We observed remarkable levels of behavioral rescue within half an

hour of treatment, reflected in the frequency, duration and extent of contractions measured during stimulus evoked swimming. Additionally, paired recordings revealed an increase in quantal content and a reduction in the number of failures. The mechanisms through which roscovitine promotes synaptic transmission are under debate and may involve either direct agonist actions (Yan et al., 2002; Cho and Meriney, 2006: Buraei et al., 2007) or through signaling pathways involving phosphorylation (Tomizawa et al., 2002; Kim and Ryan, 2010). The results from expressed P/Q- and N-type channels (Buraei et al., 2007) and frog NMJ (Cho and Meriney, 2006) both support the direct agonist action involving slowed channel deactivation. The evidence for phosphorylation independent regulation comes from a roscovitine analogue that has weak CDK inhibitor activity, but strongly promotes calcium entry (Tarr et al., 2012). Thus, roscovitine may represent an agonist for P/Q- and N-type channels, similar to BAY K analogues that act on L-type channels. Our results from P/Q-type channels expressed in HEK cells confirmed the prolongation of calcium tail currents, supporting the published effects on channel deactivation (Cho and Meriney, 2006). The augmentation of synaptic transmission, along with the motility rescue, both further the idea that administration of roscovitine or its chemical derivatives (Tarr et al., 2012) to patients with LEMS may have benefits beyond the actions on the associated lung tumor. The identification of the zebrafish P/Q mutant line now offers an ideal platform for electrophysiological assessment of the effectiveness of pharmacological derivatives in treatment of congenital LEMs.

Acknowledgments

This work was supported by grants from the NIH and MDA to P.B.; a fellowship from the NIH to M.L. The *tb204a* mutant line was generously provided by The Max Planck Institute (Tüebingen, Germany). We are grateful to Dr. Diane Lipscombe for her help with calcium channel expression clones and thank Dr. Mike Walogorsky for helping with positional cloning.

References

Buraei Z, Schofield G, Elmslie KS. Roscovitine differentially affects CaV2 and Kv channels by binding to the open state. Neuropharm. 2007; 52:883–894.

Burgess HA, Granato M. Modulation of locomotor activity in larval zebrafish during light adaptation. J Exp Biol. 2007; 210:2526–2539. [PubMed: 17601957]

Cho S, Meriney SD. The effects of presynaptic calcium channel modulation by roscovitine on transmitter release at the adult frog neuromuscular junction. Euro J Neurosci. 2006; 23:3200–3208.

Ellinor PT, Zhang J, Horne W, Tsien RW. Structural determinants of the blockade of N-type calcium channels by a peptide neurotoxin. Nature. 1994; 372:272–275. [PubMed: 7969473]

Favreau P, Gilles N, Lamthanh H, Bournaud R, Shimihara T, Bouet F, Laboute P, Letourneux Y, Menez A, Molgo J, Le Gall F. A new omega-conotoxin that targets N-type voltage sensitive calcium channels with unusual specificity. Biochemistry. 2001; 40:14567–14575. [PubMed: 11724570]

Granato M, van Eeden FJ, Schach U, Trowe T, Brand M, Furutani-Seiki M, Haffter P, Hammerschmidt M, Heisenberg CP, Jiang YJ, Kane DA, Kelsh RN, Mullins MC, Odenthal J, Nüsslein-Volhard C. Genes controlling and mediating locomotion behavior of the zebrafish embryo and larva. Development. 1996; 123:399–413. [PubMed: 9007258]

Hulsizer SC, Meriney SD, Grinnell AD. Calcium currents in presynaptic varicosities of embryonic motoneurons. Ann N Y Acad Sci. 1991; 635:424–428. [PubMed: 1660245]

Kasai H, Aosaki T, Fukuda J. Presynaptic Ca-antagonist omega-conotoxin irreversibly blocks N-type calcium channels in chick sensory neurons. Neurosci Res. 1987; 4:228–235. [PubMed: 2437502]

Katz E, Ferro PA, Cherskey BD, Sugimori M, Llinas R, Uchitel OD. Effects of calcium channel blockers on transmitter release and presynaptic currents at the frog neuromuscular junction. J Physiol. 1995; 486:695–706. [PubMed: 7473230]

Katz B, Miledi R. The timing of calcium action during neuromuscular transmission. J Physiol. 1967; 189:535–544. [PubMed: 6040160]

Kerr LM, Yoshikami D. A venom peptide with a novel presynaptic blocking action. Nature. 1984; 308:282–284. [PubMed: 6608056]

Kim SH, Ryan TA. CDK5 serves as a major control point in neurotransmitter release. Neuron. 2010; 67:797–809. [PubMed: 20826311]

Lindgren CA, Moore JW. Identification of ionic currents at presynaptic nerve endings of the lizard. J Physiol. 1989; 414:201–222. [PubMed: 2575161]

Low SE, Woods IG, Lachance M, Ryan J, Schier AF, Saint-Amant L. Touch responsiveness in zebrafish requires voltage-gated calcium channel 2.1b. J Neurophys. 2012; 102:148–159.

Lundy PM, Hamilton MG, Frew R. Pharmacological identification of a novel calcium channel in chicken brain synaptosomes. Brain Res. 1994; 643:204–210. [PubMed: 8032915]

McCleskey EW, Fox AP, Feldman DH, Cruz LJ, Olivera BM, Tsien RW, Yoshikami D. Omega-conotoxin: Direct and persistent blockade of specific types of calcium channels in neurons but not muscle. Proc Natl Acad Sci. 1987; 84:4327–4331. [PubMed: 2438698]

McDonough SI, Swartz KJ, Mintz IM, Boland LM, Bean BP. Inhibition of calcium channels in rat central and peripheral neurons by omega-conotoxin MVIIC. J Neurosci. 1996; 16:2612–2623. [PubMed: 8786437]

McDonough SI, Boland LM, Mintz IM, Bean BP. Interactions among toxins that inhibit N-type and P-type calcium channels. J Gen Physiol. 2002; 119:313–328. [PubMed: 11929883]

Mori Y, Friedrich T, Kim M, Mikami A, Nakai J, Ruth P, Bosse E, Hofmann F, Flockerzi V, Furuichi TR, Mikoshiba K, Imoto K, Tanabe T, Numa S. Primary structure and functional expression from complementary DNA of a brain calcium channel. Nature. 1991; 350:398–402. [PubMed: 1849233]

Nurullin LF, Mukhitov AR, Tsentsevytsky AN, Petrova NV, Samigullin DV, Malomouzh AI, Bukhareaeva EA, Vyskocil F, Nikolsky EE. Voltage-dependent P/Q-type calcium channels at the frog neuromuscular junction. Physiol Res. 2011; 60:815–823. [PubMed: 21812515]

Protti DA, Reisin R, Mackinley TA, Uchitel OD. Calcium channel blockers and transmitter release at the normal human neuromuscular junction. Neurology. 1996; 46:1391–1396. [PubMed: 8628488]

Plummer MR, Logothetis DE, Hess P. Elementary properties and pharmacological sensitivities of calcium channels in mammalian peripheral neurons. Neuron. 1989; 2:1453–1463. [PubMed: 2560643]

Regan LJ, Sah DW, Bean BP. Calcium channels in rat central and peripheral neurons: High threshold current resistant to dihydropyridine blockers and omega-conotoxin. Neuron. 1991; 6:269–280. [PubMed: 1847065]

Regher W, Mintz I. Participation of multiple calcium channel types in transmission at single climbing fiber to Purkinje cell synapses. Neuron. 1994; 12:605–613. [PubMed: 8155322]

Robitaille R, Adler EM, Charlton MP. Strategic localization of calcium channels at transmitter release sites of frog neuromuscular synapses. Neuron. 1990; 5:773–779. [PubMed: 1980068]

Quartel A, Turbeville S, Lounsbury D. Current therapy for Lambert-Eaton syndrome: development of 3,4-diaminopyridine phosphate salt as first-line symptom treatment. Current Medical Res & Opinion. 2010; 26:1363–1375.

Sano K, Enomoto K, Maeno T. Effects of synthetic ω-conotoxin, a new type calcium antagonist, on frog and mouse neuromuscular transmission. Eur J Pharmacology. 1987; 141:235–241.

Senderowicz AM. Novel small molecule cyclin-dependent kinase modulators in human clinical trials. Cancer Biol Ther. 2003; 2:S84eS95. [PubMed: 14508085]

Sheng ZH, Rettig J, Cook T, Catterall WA. Calcium-dependent interaction of N-type calcium channels with the synaptic core complex. Nature. 1996; 379:451–454. [PubMed: 8559250]

Siri R, Uchitel OD. Calcium channels couple to neurotransmitter release at neonatal rat neuromuscular junctions. J Physiol. 1999; 514:533–540. [PubMed: 9852333]

Tarr T, Valdomir G, Liang M, Wipf P, Meriney SD. New calcium channel agonists as potential therapeutics in Lambert-Eaton myasthenic syndrome and other neuromuscular diseases. Ann. N. Y. Acad. Sci. 2012; 1275(1):85–91. [PubMed: 23278582]

Thaler C, Li W, Brehm P. Calcium channel isoforms underlying synaptic transmission at embryonic *Xenopus* neuromuscular junctions. J Neurosci. 2001; 21:412–422. [PubMed: 11160422]

Tomizawa K, Ohta J, Matsushita M, Moriwaki A, Li S, Takei K, Matsui H. Cdk5/p35 regulates neurotransmitter release through phosphorylation and downregulation of P/Q-type voltage-dependent calcium channel activity. J Neurosci. 2002; 22:2590–2597. [PubMed: 11923424]

Uchitel O, Protti D, Sanchez V, Chersky B, Sugimori M, LLinas R. P-type voltage-dependent calcium channel mediates presynaptic calcium influx and transmitter release in mammalian synapses. Proc Natl Acad Sci. 1992; 89:3330–3333. [PubMed: 1348859]

Urbano FJ, Rosato-Siri MD, Uchitel OD. Calcium channels involved in neurotransmitter release at adult, neonatal and P/Q-type deficient neuromuscular junctions. Mol Membr Biol. 2002; 1:293–300. [PubMed: 12512776]

Wen H, Brehm P. Paired motor neuron-muscle recordings in zebrafish test the receptor blockade model for shaping synaptic current. J Neurosci. 2005; 25:8104–8111. [PubMed: 16135768]

Wen H, Brehm P. Paired patch clamp recordings from motor-neuron and target skeletal muscle in zebrafish. J Vis Exp Nov. 2010; 20(45):2351. pii.

Wen H, Linhoff MW, McGinley MJ, Li GL, Corson GM, Mandel G, Brehm P. Distinct roles for two synaptotagmin isoforms in synchronous and asynchronous transmitter release at zebrafish neuromuscular junction. Proc Natl Acad Sci. 2011; 107:13906–13911. [PubMed: 20643933]

Yan Z, Chi P, Bibb JA, Ryan TA, Greengard P. Roscovitine: a novel regulator of P/Q-type calcium channels and transmitter release in central neurons. J Physiol. 2002; 540(Pt 3):761–770. [PubMed: 11986366]

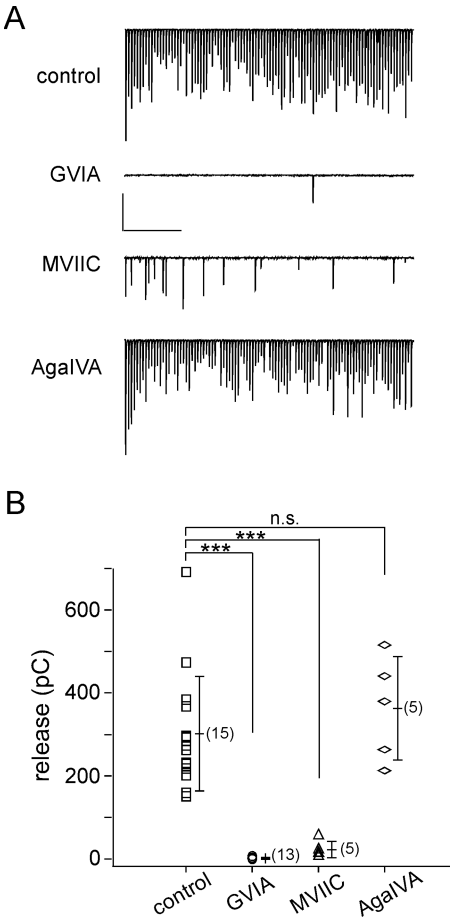

Figure 1.

Paired motor neuron-muscle recordings indicate N-type calcium channel involvement in zebrafish neuromuscular transmission. (A) Postsynaptic recordings of EPCs in response to a 1 sec, 100 Hz train of action potentials elicited in the motor neuron soma. Untreated fish are compared to individual fish treated with 1 μM ω-conotoxin GVIA, 1 μM ω-conotoxin MVIIC or 2 μM ω-agatoxin IVA. Vertical calibration corresponds to 1 nA for ω-conotoxin GVIA and ω-conotoxin MVIIC and 2 nA for control and ω-Agatoxin IVA. Horizontal calibration corresponds to 200 msec. (B) Scatter plot of total release from individual experiments, n value (in parenthesis), along with cumulative mean ± S.D. for each treatment. The total release was quantitated as charge entry during the 1 sec, 100 Hz train by integrating the postsynaptic current, as previously described (Wen et al., 2011). *** corresponds to $p < 0.001$. n.s. corresponds to $p = 0.38$.

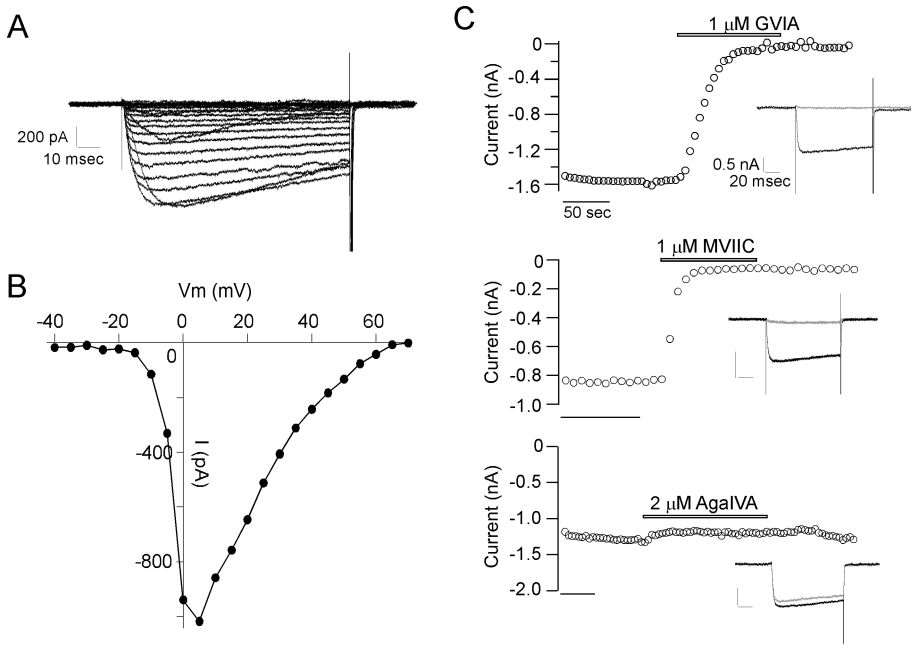

Figure 2.

Pharmacology of the zebrafish N-type calcium channel expressed in HEK293T cells. (A) Sample current traces in 5 mV depolarizing increments from a -80 mV holding potential. The recordings were performed in 1 mM Ba^{2+} and traces were leak subtracted using p/10 protocol. (B) Current-voltage relations of the leak subtracted Ba^{2+} current for the recording shown in A. (C) Examples of time-dependent block of Ba^{2+} current in response to the three different indicated toxins. Each point corresponds to a measurement of inward current at +10 mV. The horizontal bar above the graph indicates the time during which the toxin was applied to the cell. The insets show the maximal inward current prior to toxin application (black) and after maximal block was achieved (grey). Calibration bars are labeled in the top panel.

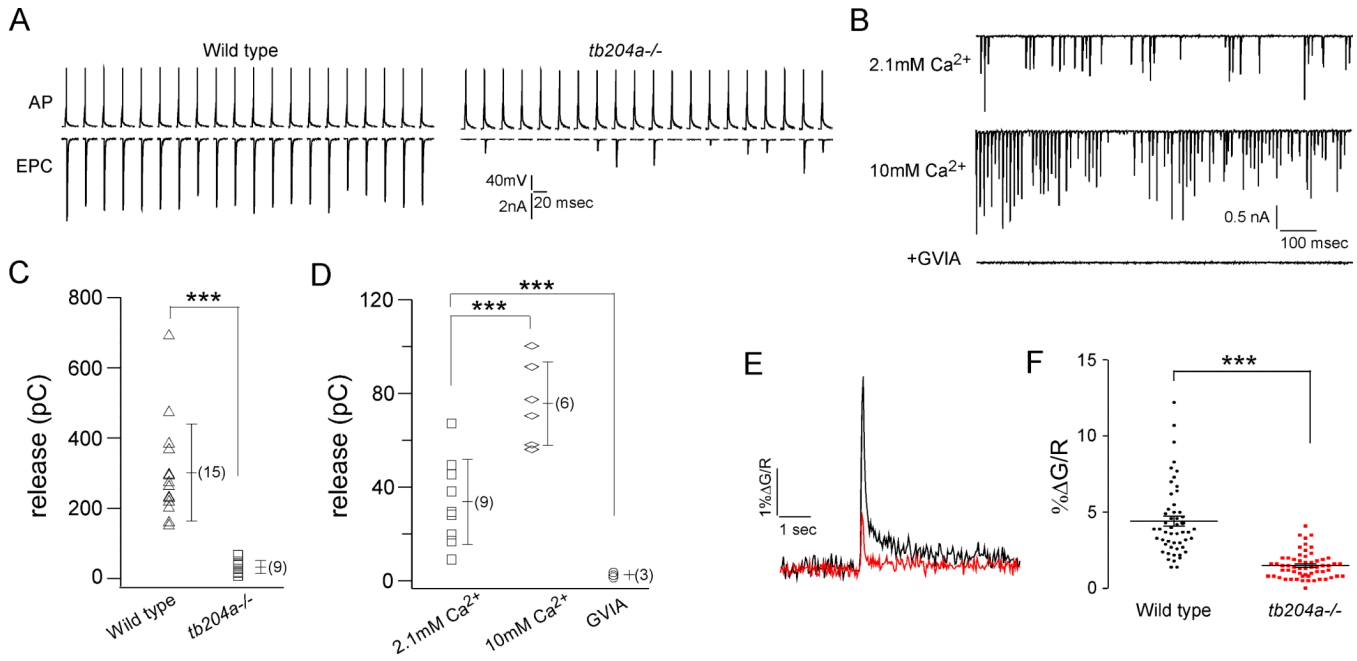

Figure 3.

Compromised neuromuscular transmission in *tb204a* mutant fish. (A) Paired CaP motor neuron-skeletal muscle recordings from a wild type and *tb204a* mutant fish during 1 Hz stimulation. The presynaptic action potential (AP) and associated EPC are shown. The recordings shown are discontinuous for the purpose of presentation. (B) Postsynaptic recordings of the *tb204a* mutant during 1 sec, 100 Hz stimulation showing decreased failures and increased EPC amplitude when external calcium was elevated from 2.1 mM to 10 mM. All residual postsynaptic activity was eliminated by addition of 1 μM ω-conotoxin GVIA. (C) Scatter plots of individual experiments comparing wild type and *tb204a* mutants release, measured as total charge, during a 1 sec, 100 Hz stimulus train. Each point represents the measurement from a single experiment. Overall mean ± S.D. and n value (in parenthesis) are indicated. (D) Scatter plot of individual experiments comparing the total charge obtained for *tb204a* mutants in 2.1 mM Ca^{2+}, 10 mM Ca^{2+}, and 1 μM ω-conotoxin GVIA. *** Indicates $p < 0.001$. (E) Fluo-5F measurements of calcium response in the presynaptic boutons of wild type and *tb204a* mutant fish during a 100 msec, 100 Hz stimulus train. Each trace represents the average responses of wild type (black, 4 fish, 52 boutons) and *tb204a* (red, 4 fish, 59 boutons) boutons. The change in Fluo-5F signal (ΔG) was normalized to the fluorescent fill (R) and expressed in arbitrary units. (F) Comparison of normalized Fluo-5F signal for individual bouton in wild type and *tb204a* fish. The overall mean values are shown and *** represents $p < 0.001$.

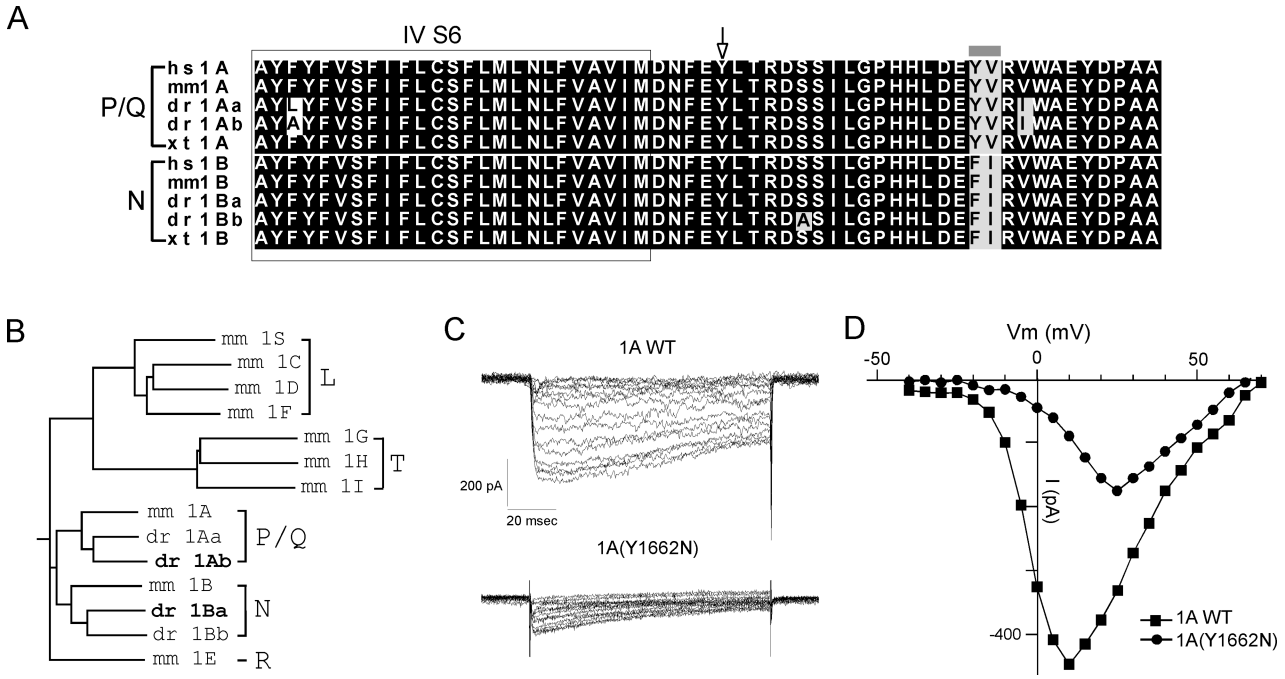

Figure 4.

Cloning and expression of zebrafish CACNA1Ab P/Q-type calcium channel in HEK293T cells. (A) Alignments of calcium channel sequences from various species in the region corresponding to the *tb204a* point mutation. The sequence comparisons represent the S6 membrane spanning region in Domain IV (in box) and intracellular region for both P/Q- and N-type calcium channels in human (hs), mouse (mm), fish (dr) and *Xenopus* (xt). Zebrafish has two genes for P/Q-type (1Aa & 1Ab) and N-type channel (1Ba & 1Bb). Identical residues are shaded black and similar residues are shaded in gray. The gray bar denotes a pair of residues that can be used to distinguish N- and P/Q-type channels. The arrow denotes the location of the *tb204a* point mutation from tyrosine (Y) to asparagine (N). (B) A dendrogram showing the clustering of the annotated N- and P/Q-type genes for zebrafish with the respective mouse voltage-dependent calcium channel sub-groups according to their sequence similarity. The dendrogram was generated by CLUSTRAL W program. The zebrafish calcium channel isoforms in this study are in bold. (C) Sample Ba^{2+} currents from wild type (top) and mutant (bottom) P/Q-type channels expressed in HEK293T cells. The cells were held at -80 mV and incrementing steps of 5 mV were applied. (D) The current-voltage relations for the wild type (square) and mutant (circle) Ba^{2+} currents shown in C.

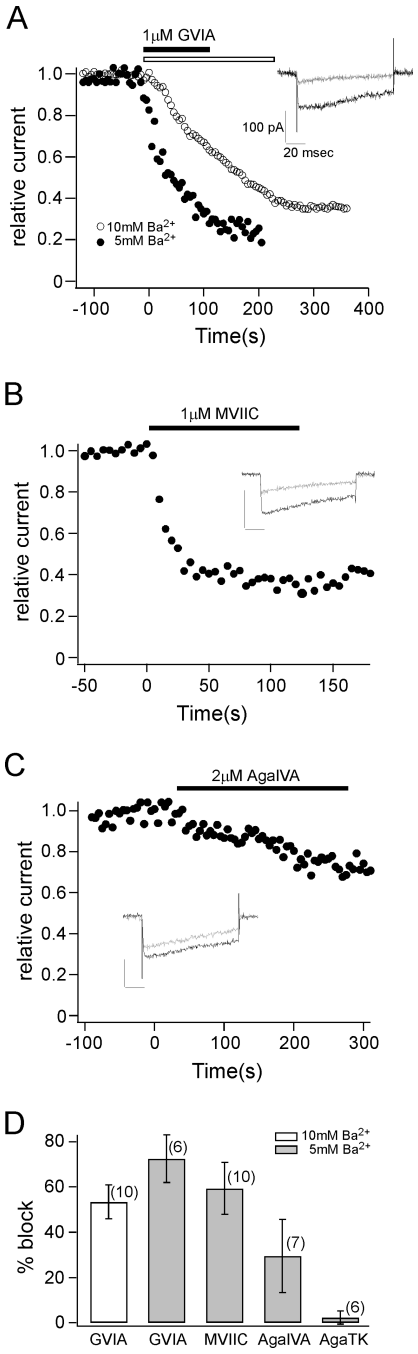

Figure 5.

Pharmacological profile of the zebrafish CACNA1Ab P/Q-type calcium channel expressed in HEK293T cells. (A) Representative recordings showing comparison of the block by 1 μM ω-conotoxin GVIA in 5 mM (filled symbols) and 10 mM (open symbols) Ba^{2+}. The block is represented by the time-dependent reduction from pre-block peak current amplitude. Each time point was taken at 5 sec interval. The time of pressure application is indicated in each divalent concentration by the horizontal bars. The inset shows the Ba^{2+} current recorded pre-application (dark trace) and post-application (light trace) of ω-conotoxin GVIA. The test voltage steps corresponded to +10 mV from a holding potential of -80 mV. (B) The block by 1 μM ω-conotoxin MVIIC shown in the same manner as A. (C) The block by 2 μM ω-

Agatoxin IVA is shown in the same manner as A. (D) Comparison of the current block by different toxins. Average percentage of block and n value (in parenthesis) for each condition are shown.

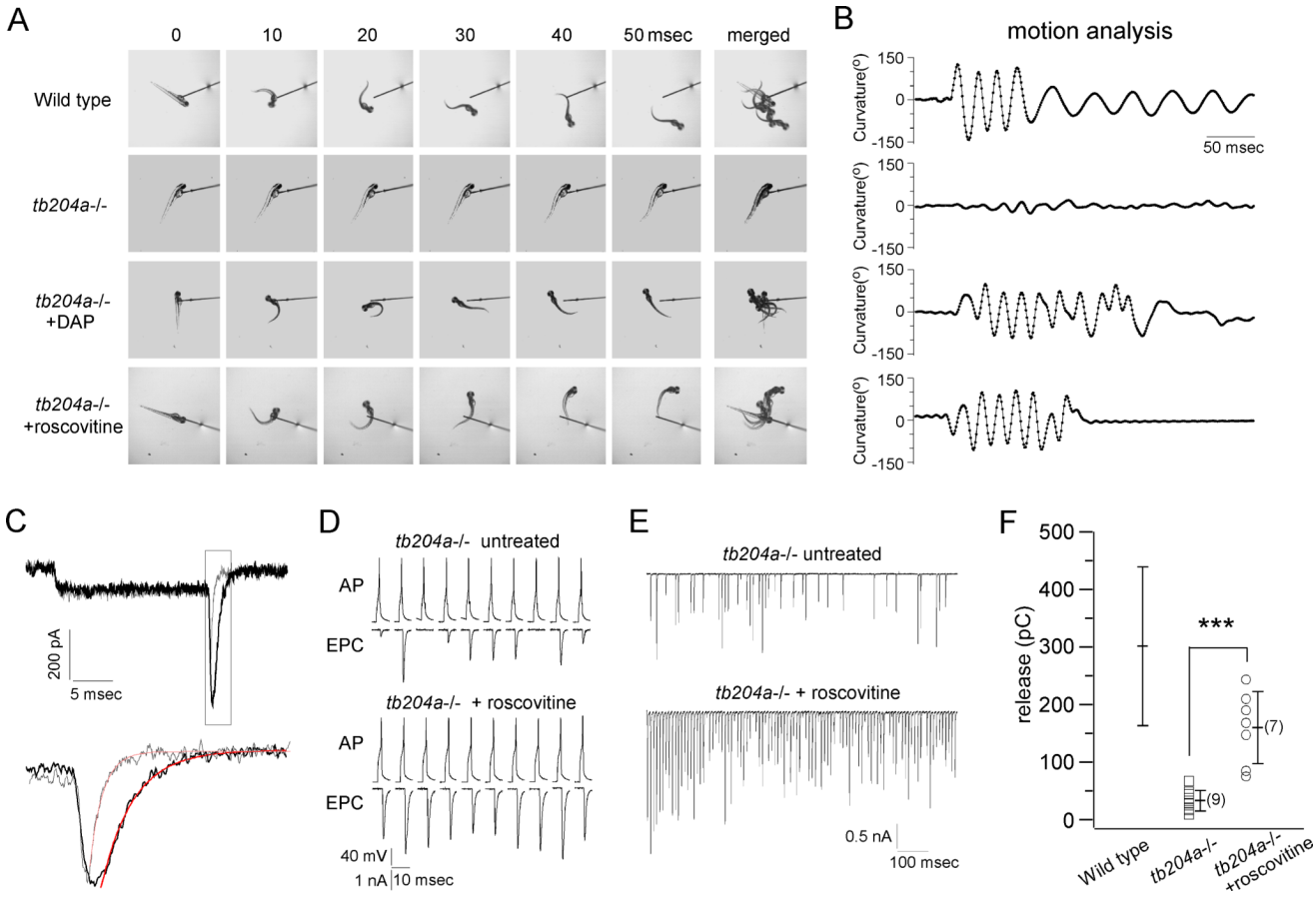

Figure 6.

Roscovitine rescues *tb204a* mutant phenotype. (A) Comparison of the touch responses from wild type, *tb204a* mutant, and *tb204a* mutant following treatment with either 200 μM DAP or 100 μM roscovitine. Six consecutive still images taken at 10 msec intervals following mechanical stimulation are shown. Merged images are shown at the end of each row. (B) Motion analysis of mechanical induced escape responses using Flote software. The curvature reflects the degree of body axis bend associated with the swimming. (C) Barium currents recorded from zebrafish P/Q-type calcium channels expressed in HEK cells before (gray) and during (black) application of roscovitine. The voltage was stepped from -80mV to +40mV for 20 msec before returning to -80mV. Tail currents shown in the box are expanded in the lower traces and the fits to a single exponential curve shown in red. (D) Paired recording traces from untreated and roscovitine treated *tb204a* mutant fish are shown for 1 Hz stimulation. (E) Paired recording traces from an untreated *tb204a* mutant and a roscovitine treated mutant fish during 1 sec, 100 Hz stimulation. (F) Comparison of total release during 1 sec, 100 Hz stimulation from untreated and roscovitine treated *tb204a* mutant fish. Each symbol corresponds to the value obtained for individual experiments. The overall mean, S.D. and n value (in parenthesis) for each condition are shown. The mean ± S.D. previously shown in Figures 1 and 3 for wild type fish are indicated for the purpose of comparison. ***indicates $p < 0.001$.